

UC Berkeley

UC Berkeley Previously Published Works

Title

Spatiotemporal Crossover between Low- and High-Temperature Dynamical Regimes in the Quantum Heisenberg Magnet

Permalink

<https://escholarship.org/uc/item/8cx3w9cb>

Authors

Dupont, Maxime

Sherman, Nicholas E

Moore, Joel E

Publication Date

2021-04-27

Peer reviewed

Spatiotemporal crossover between low- and high-temperature dynamical regimes in the quantum Heisenberg magnet

Maxime Dupont, Nicholas E. Sherman, and Joel E. Moore

*Department of Physics, University of California, Berkeley, California 94720, USA and
Materials Sciences Division, Lawrence Berkeley National Laboratory, Berkeley, California 94720, USA*

The stranglehold of low temperatures on fascinating quantum phenomena in one-dimensional quantum magnets has been challenged recently by the discovery of anomalous spin transport at high temperatures. Whereas both regimes have been investigated separately, no study has attempted to reconcile them. For instance, the paradigmatic quantum Heisenberg spin-1/2 chain falls at low-temperature within the Tomonaga-Luttinger liquid framework, while its high-temperature dynamics is superdiffusive and relates to the Kardar-Parisi-Zhang universality class in 1 + 1 dimensions. This work aims at reconciling the two regimes. Building on large-scale matrix product state simulations, we find that they are connected by a temperature-dependent spatiotemporal crossover. As the temperature T is reduced, we show that the onset of superdiffusion takes place at longer length and time scales $\propto 1/T$. This prediction has direct consequences for experiments including nuclear magnetic resonance: it is consistent with earlier measurements on the nearly ideal Heisenberg $S = 1/2$ chain compound Sr_2CuO_3 yet calls for new and dedicated experiments.

Introduction.— At low temperatures, reduced spatial dimensionality greatly enhances quantum fluctuations in physical systems, giving rise to exotic properties. In that regard, one-dimensional (1D) quantum many-body systems have always been influential and generically fall into two classes [1, 2]: on the one hand, gapless low-energy excitations described in the framework of Tomonaga-Luttinger liquid (TLL), and on the other, a gapped behavior. Theoretical predictions have been intensively checked by experiments in various contexts, ranging from ultra-cold atom setups to quantum magnets [3, 4].

At energy $\hbar\omega \ll k_B T$, the physics is usually thought of in terms of thermal rather than quantum effects. This regime had not been thought to hold phenomena as compelling as its low-temperature counterpart until very recently. Indeed, recent theoretical progress suggests that the equilibrium and out-of-equilibrium dynamics of some 1D quantum systems can exhibit peculiar behaviors and contain information about the intrinsic quantum features, even at very high temperatures [5–7].

While such many-particle systems are governed at the microscopic level by the Schrödinger equation, they display in the long-time and long-wavelength limits an emergent coarse-grained hydrodynamic behavior. An analogy can be made with classical fluid dynamics: one does not describe individual particles with Newton’s laws of motion but relies instead on phenomenological continuous differential equations, ideally more amenable. The derivation of hydrodynamic equations is based essentially on continuity equations of conserved quantities (e.g., mass, energy, etc.), assuming local equilibrium [8].

Quantum systems also possess conservation laws, and depending on those, one expects the emergence of different kinds of coarse-grained hydrodynamic descriptions. Singularly in 1D, a class of quantum systems – known as integrable – has an infinite set of nontrivial conserved quantities which can lead to anomalous dynamical behaviors [5–7, 9–34].

Integrable systems are typically described by very fine-tuned models but some of them can be reliably realized in the lab (e.g., the Lieb-Liniger model representing a gas of

one-dimensional bosons with contact repulsion [35, 36]) and found with high fidelity in nature (e.g., the spin-1/2 Heisenberg chain of magnetic moments coupled by a nearest-neighbor exchange interaction [2]). In that context, some of the theoretical predictions have been successfully tested on 1D cloud of trapped ^{87}Rb [37, 38] and ^7Li [39] atoms for out-of-equilibrium dynamics and by neutron scattering on the quantum magnet KCuF_3 at thermal equilibrium [34].

In the case of quantum magnets, it has been numerically conjectured, based on microscopic simulations, that in the limit of infinite temperature, the spin dynamics of the $S = 1/2$ Heisenberg chain is anomalous and belongs to the Kardar-Parisi-Zhang (KPZ) universality class in 1 + 1 dimensions [20, 40]. It is characterized by a dynamical exponent $z = 3/2$, controlling the length-time scaling of the dynamical properties. This exponent has been recently observed in the high-temperature neutron spectrum of KCuF_3 [34], which is directly proportional to the dynamical structure factor, probing spin-spin correlations.

Here, we seek to reconcile the low-temperature physics of the $S = 1/2$ Heisenberg chain, falling within the gapless TLL category, with the recently found infinite-temperature KPZ hydrodynamics. Whereas both regimes have been studied independently, no work has attempted to bring them together. In this Letter, we precisely define the long-time and long-wavelength limits for the emergence of anomalous dynamics versus the temperature. We find that these limits define a spatiotemporal crossover beyond which hydrodynamics take place. As the temperature is lowered, the crossover is pushed towards infinity and eventually disappears at exactly zero temperature, see Fig. 1. This scenario allows one to recover the well-known zero temperature results where KPZ hydrodynamics is absent. Moreover, because experimental dynamical condensed matter probes such as neutron scattering or nuclear magnetic resonance (NMR) work for all practical purposes at a finite frequency and finite temperatures, it is paramount to better understand and quantitatively define the theoretical limits. We discuss the implication of our results for experiments and confront our findings to earlier high-temperature NMR ex-

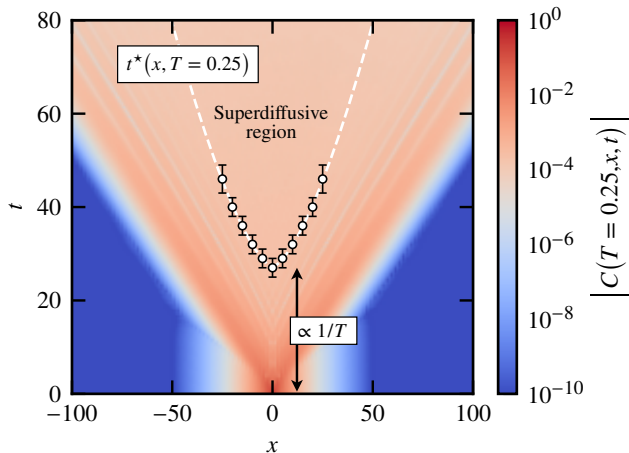


FIG. 1. Log-scale intensity plot of the Euclidean norm of the spin-spin correlation (2) at $T = 0.25$. Simulation obtained for $L = 256$ with $\chi = 1024$. The goal of this work is to determine and study the superdiffusive region delimited by the spatiotemporal crossover t^* of Eq. (3) versus the temperature (white circles and dashed white line). As the temperature is decreased, we find that the superdiffusive region is shifted vertically to longer and longer times by a factor $\propto 1/T$, and eventually disappear at exactly zero temperature.

periments on the nearly ideal Heisenberg spin-1/2 compound Sr_2CuO_3 [41].

Model and method.— The 1D spin-1/2 Heisenberg model is described by the lattice Hamiltonian,

$$\hat{\mathcal{H}} = J \sum_j \hat{\mathbf{S}}_j \cdot \hat{\mathbf{S}}_{j+1}, \quad (1)$$

with $\hat{\mathbf{S}}_j = (\hat{S}_j^x, \hat{S}_j^y, \hat{S}_j^z)$ and $J > 0$ the nearest-neighbor antiferromagnetic exchange. To investigate the thermal equilibrium spin dynamics, we consider the time-dependent spin-spin correlation function,

$$C(T, x, t) = \text{tr}(\hat{\mathbf{S}}_x(t) \cdot \hat{\mathbf{S}}_0(0) \hat{\rho}_T) \in \mathbb{C}, \quad (2)$$

with $\hat{\rho}_T = e^{-\hat{\mathcal{H}}/k_B T} / \text{tr}(e^{-\hat{\mathcal{H}}/k_B T})$ the thermal density matrix of the system at temperature T and $\hat{\mathbf{S}}_j(t) = e^{i\hat{\mathcal{H}}t/\hbar} \hat{\mathbf{S}}_j e^{-i\hat{\mathcal{H}}t/\hbar}$ the time-dependent spin operator in the Heisenberg picture. We set $J = k_B = \hbar = 1$ in the following. We compute the correlation function (2) based on a numerical matrix product state (MPS) approach [42, 43] where we represent the mixed state as a pure state in an enlarged Hilbert space [44, 45]. We use the time-evolving block decimation algorithm [46] along with a fourth-order Trotter decomposition [47] to handle the exponential operators [48]. To ensure convergence of the numerical data, we study in the Supplementary Information (SI) the effect of the bond dimension χ of the MPS, which is the control parameter of the simulations (larger is better, but computationally more expensive) [49].

At fixed distance x and temperature T , the hydrodynamics regime is characterized by an algebraic decay of the Euclidean

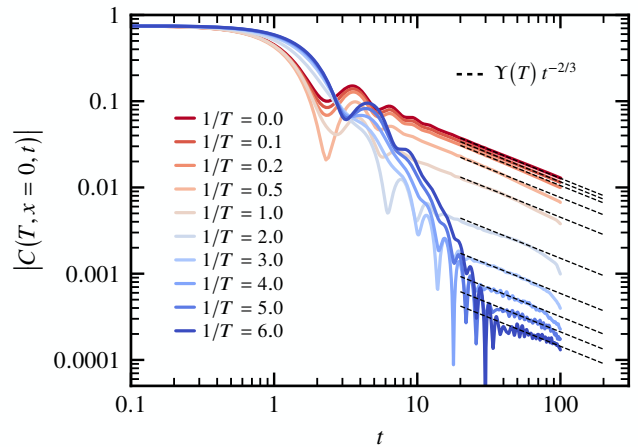


FIG. 2. Time dependence of the norm of the spin-spin correlation (2) at $x = 0$ for various temperatures T . Simulations obtained for $L = 256$ with $\chi = 1024$. At long time, it displays an algebraic decay with time, according to Eq. (3). It is well-fitted by the form $\Upsilon(T) t^{-2/3}$ with $\Upsilon(T)$ a temperature-dependent prefactor decreasing with the temperature reported in Fig. 3(b). The deviation from the genuine power-law at long-time is the result of the bond dimension being too small [49].

norm of the spin-spin correlation (2) function at long time,

$$|C(T, x, t)| \propto t^{-1/z} \quad \text{for } t \gtrsim t^*(x, T), \quad (3)$$

with z the dynamical exponent. The long-time limit is denoted by the crossover time t^* which we aim to identify, see Fig. 1. Depending on the microscopic model, three values for the exponent z have been reported for 1D quantum magnets: $z = 3/2$ corresponding to superdiffusion, $z = 1$ for ballistic and $z = 2$ for diffusion [24, 25]. Superdiffusion is expected for the isotropic spin-1/2 Heisenberg model of Eq. (1).

Autocorrelation.— We first consider the autocorrelation function ($x = 0$) versus time for different temperatures, as plotted in Fig. 2. Two regimes are clearly visible, delimited by the crossover time $t^*(x = 0, T)$. Beyond the crossover time and for all temperatures, one finds the expected power-law decay $\propto t^{-2/3}$ of superdiffusive hydrodynamics. Note that the rapid change of slope from the genuine power-law, at the longest times displayed, is the result of the bond dimension being too small and not a physical effect [49].

With high-temperature physics beyond t^* , one can suspect low-temperature features at shorter times. For instance, the oscillating behavior observed in the norm of the autocorrelation is reminiscent of a change of sign in the real and imaginary part [49], signaling antiferromagnetic correlations as the temperature is lowered. The long-time asymptotic of $C(T = 0, x = 0, t)$ have been studied at exactly zero temperature [50, 51]. It is composed by several power-law decaying contributions with the slowest one being $\propto t^{-1}$ (up to logarithmic corrections inherent to the isotropic spin-1/2 Heisenberg antiferromagnet [52–59]). We cannot identify this regime in Fig. 2, which we attribute to insufficiently low temperatures, see the SI for additional data [49].

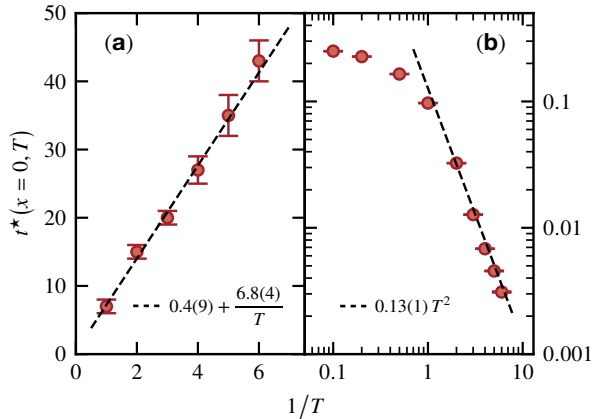


FIG. 3. The data points are extracted from Fig. 2. (a) Temperature dependence of the crossover timescale $t^*(x=0, T)$ beyond which the algebraic decay $\propto t^{-2/3}$ for superdiffusive hydrodynamics emerges, see Eq. (3). It shows a linear dependence with the inverse temperature (dashed line). (b) Temperature dependence of the prefactor $\Upsilon(T)$ of the algebraic decay $\propto t^{-2/3}$ for superdiffusive hydrodynamics. At low temperatures $T \lesssim 1$, it follows a quadratic dependence $\propto T^2$ (dashed line).

We now turn our attention to the temperature dependence of the crossover time $t^*(x=0, T)$. It is plotted in Fig. 3(a) versus the inverse temperature and shows a linear dependence. It can be understood as follows. It is well-known that a finite temperature induces a thermal correlation length ξ which diverges as $T \rightarrow 0$ as $\propto u/T$ (up to logarithmic corrections) with u the velocity of low-energy excitations in the spin-1/2 chain [53]. Moreover, the dynamical correlation function (2) can also be thought of as measuring the spreading of a spin excitation. In this picture, the system behaves like a TLL for $t \lesssim \xi/u$, which can be identified as the crossover time $t^*(x=0, T) \propto 1/T$. Hence, the onset of superdiffusive hydrodynamics simply takes place as the low-energy physics gets suppressed by the finite temperature. It is only at zero temperature that the system is strictly critical and thus does not display any sign of anomalous high-energy dynamics. In addition to the linear dependence with $\propto 1/T$, there is an $O(1)$ constant in Fig. 3(a) which coincides with the very short-time dynamics where $|C(T, x=0, t \approx 0)| \approx 0.75$.

At infinite temperature, it has been established that the dynamics belong to the 1+1 KPZ universality class [20, 40], as it shows the same scaling laws as appear in the KPZ equation itself: $\partial_t h = \frac{1}{2}\lambda(\partial_x h)^2 + \nu\partial_x^2 h + \sigma\eta$ with $h \equiv h(x, t)$, $\eta \equiv \eta(x, t)$ a normalized Gaussian white noise, and λ, ν, σ parameters. It is a Langevin equation, with no quantum roots – and which makes the observation of its physics in a quantum magnet rather puzzling. In the right limits, the noise-averaged slope correlations behave as [60],

$$C_{\text{KPZ}}(x, t) \approx \left(\frac{\sigma^2}{2\nu}\right) (\sqrt{2}\lambda t)^{-2/3} f_{\text{KPZ}} \left[x (\sqrt{2}\lambda t)^{-2/3} \right], \quad (4)$$

with f_{KPZ} the KPZ scaling function [61]. The numerical obser-

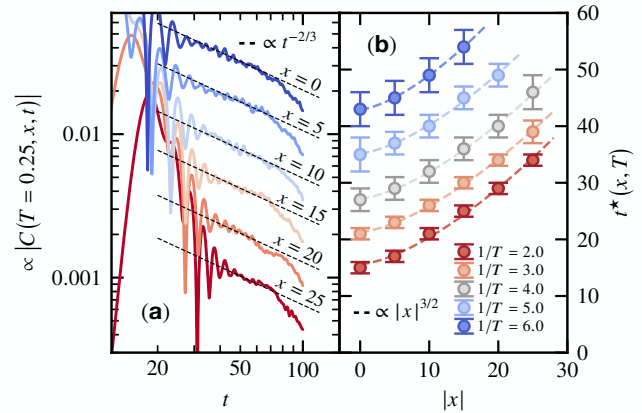


FIG. 4. (a) Time dependence of the norm of the spin-spin correlation (2) at $T = 0.25$ for various distances x . Simulations obtained for $L = 256$ with $\chi = 1024$. The curves have been shifted vertically for visibility. At long time, it displays an algebraic decay with time, according to Eq. (3), well-fitted by the form $\propto t^{-2/3}$. The deviation from the genuine power-law at long time is the result of the bond dimension being too small [49]. (b) Spatial dependence of the crossover time $t^*(x, T)$ beyond which the algebraic decay $\propto t^{-2/3}$ for superdiffusive hydrodynamics emerges, see Eq. (3). The dashed lines are fits of the form $A + B|x|^{3/2}$ with $A \equiv t^*(0, T)$ and $B = 0.17(3)$ found to be temperature-independent.

vation of the scaling (4) for the Heisenberg spin chain through the spin-spin correlation (2) served as a conjecture regarding the nature of its dynamics [20]. A theoretical scenario for how KPZ hydrodynamics emerges in the Heisenberg chain has been advanced [30]. A relation between the parameters of the KPZ equation with those of the microscopic quantum model has been proposed [26]. Here, by identifying the prefactor of $C_{\text{KPZ}}(x=0, t)$ in Eq. (4) with the prefactor $\Upsilon(T)$ of the power-law decay $\propto t^{-2/3}$ shown in Fig. 3(b), we are able to report on the temperature dependence of the parameters. The high-temperature data points are compatible with Ref. 26. In addition, for $T \lesssim 1$, we find that $\Upsilon(T) = 0.13(1)T^2$, and therefore that $\frac{\sigma^2}{2\nu} (\sqrt{2}\lambda)^{-2/3} f_{\text{KPZ}}(0) \propto T^2$. We argue in the following that this behavior is compatible with earlier NMR experiments on Sr_2CuO_3 [41, 49].

The definition of the crossover time t^* in Eq. (3) for the onset of superdiffusion is related to the power-law dependence $\propto t^{-2/3}$ and not f_{KPZ} of Eq. (4). It is well-known that unambiguously identifying the scaling function from microscopic simulations with f_{KPZ} requires great numerical precision and long-time data for all distances x [20]. This is beyond the capability of our simulations at low temperatures. Instead, we consider the spatial dependence of t^* for $|x| > 0$.

Spatiotemporal crossover.— The time-dependent spin-spin correlation function (2) is associated with a light-cone structure and we therefore expect $t^*(x, T)$ to be an increasing function with the distance $|x|$. It is verified in Fig. 4(a) where we plot its time dependence at fixed temperature ($T = 0.25$). As $|x|$ increases, the onset of superdiffusion takes place at longer and longer times, and we display the crossover timescale in

Fig. 4(b) for different temperatures. Because we can only reliably estimate it for $|x| \lesssim 30$, it is difficult to draw a definite conclusion on its scaling. Nevertheless it is compatible with a superdiffusive length-time scaling of the form,

$$t^*(x, T) = 0.4(9) + \frac{6.8(4)}{T} + 0.17(3) |x|^{3/2}, \quad (5)$$

with the first two terms obtained from the $t^*(x=0, T)$ data, see Fig. 3(a). The prefactor of $|x|^{3/2}$ is found independent of the temperature. The reported numerical parameters are obtained by least-square fitting. The spatiotemporal crossover time (5) is plotted on top of the norm of the spin-spin correlation in Fig. 1 for $T = 0.25$. Note that based on this picture, we expect logarithmic corrections for the temperature dependence, but they are not detectable from our simulations.

Experimental consequences.— Although we have focused on the norm of the spin-spin correlation (2), we find that $|\Im C(T, x, t)| \ll |\Re C(T, x, t)|$ for $t \gtrsim t^*$, and that the superdiffusive power-law $\propto t^{-2/3}$ only holds for the real part [49], which therefore hosts the relevant high-temperature physics. Thus, the existence of a finite spatiotemporal crossover $t^*(x, T)$ in the form of Eq. (5) confirms that superdiffusive hydrodynamics is within the experimentally relevant window of parameters with respect to temperatures, time and length scales for quantities involving $\Re C(T, x, t)$. For instance, it was observed by neutron scattering in the limit of small momentum and vanishing frequency [34], which probes the Fourier transform to momentum and frequency spaces of $C(T, x, t)$.

Another promising experimental technique for investigating high-temperature hydrodynamics is NMR, which has been successfully used to characterize the low-temperature TLL regime in numerous spin compounds [59, 62–69]. Nuclear spins are polarized via a static magnetic field (ideally weak) and then perturbed by an electromagnetic pulse of frequency ω_0 , chosen to target specific nuclei as per the Zeeman splitting. Following the perturbation, the nuclear spins relax over time with an energy transfer to the electrons. When the nuclear and electronic spins belong to the same atom, the relaxation rate is related to the autocorrelation function, $1/T_1 \sim \int_0^{1/\omega_0} \Re C(T, x=0, t) dt$ [70–72]. With ω_0 of the order of a few mK, it usually leads to a frequency-independent $1/T_1$ as long as the correlation decays quickly enough. Here, the hydrodynamics regime should lead instead to $1/T_1 \propto \omega_0^{1/z-1}$ and give access to z in the right frequency regime. According to Eq. (5), one should have $\omega_0 \ll T$, which considering the range of ω_0 , is fulfilled down to quite low temperatures.

In fact, a power-law behavior of the form $1/T_1 \propto \omega_0^{-\alpha}$ has been reported in the nearly ideal spin-1/2 Heisenberg antiferromagnet Sr_2CuO_3 ($J \approx 2200$ K) at $T = 295$ K a couple of decades ago [41]. NMR was performed on the ^{17}O , coupled symmetrically to the Cu^{2+} carrying the relevant electronic spin, which filtered out the $q = \pm\pi$ contributions in the $1/T_1$ due to form factors, but not the long-wavelength modes $q = 0$ holding hydrodynamics. Although the measurement accuracy was not sufficiently precise to extract the exponent α , the results are

compatible with $\alpha \approx 0.33$, which corresponds to $z = 3/2$ [49]. In addition, the authors find that at fixed frequency, the NMR relaxation rate may be approximated by an empirical form $1/T_1 T \approx a + bT$ for $T \ll J$ with a and b fitting constants. When dropping a , this is compatible with $Y(T) \propto T^2$ reported in Fig. 3(b) [49], which relates to the temperature dependence of the parameters of the KPZ equation.

Today's theoretical understanding of the dynamics of 1D quantum systems and our results call for new NMR experiments on spin chains at high temperatures. It would provide a complementary probe to neutron scattering [34] to access anomalous spin transport in quantum materials.

Conclusion.— Building on large-scale MPS calculations, we reconciled the well-established low-temperature dynamics of the quantum Heisenberg spin-1/2 chain with the recently predicted high-temperature superdiffusive regime related to KPZ hydrodynamics. We have found that both coexist, and the transition from one to the other takes the form of a spatiotemporal crossover. The crossover is controlled by the temperature: as the temperature is lowered, the growing quantum correlations between degrees of freedom push the onset of superdiffusion to longer length and time scales as $\propto 1/T$. We also reported on the temperature dependence of the parameters of the KPZ equation, which should provide useful guidance in relating them to the microscopic parameters of the quantum model. We also showed that only the real part of the spin-spin correlations holds the superdiffusive hydrodynamics. Finally, we discussed the experimental consequences of our results for condensed matter probes. We motivated NMR experiments as a great way to measure spin transport in quantum materials and showed that earlier results are compatible with the current theoretical understanding yet calling for new experiments in quantum spin chains. Because NMR requires the use of a static magnetic field to polarize the nuclear spins, it would be insightful to study the effect of this perturbation on the dynamics of the $S = 1/2$ Heisenberg chain studied in this work. We believe that it would induce another crossover from superdiffusion to ballistic dynamics, which needs to be characterized.

Acknowledgments.— We gratefully acknowledge G.E. Granroth, S.E. Nagler, A. Scheie, M.B. Stone, and D.A. Tennant for collaborations on related works. M.D. acknowledges correspondence with J. De Nardis. M.D. was supported by the U.S. Department of Energy, Office of Science, Office of Basic Energy Sciences, Materials Sciences and Engineering Division under Contract No. DE-AC02-05-CH11231 through the Scientific Discovery through Advanced Computing (SciDAC) program (KC23DAC Topological and Correlated Matter via Tensor Networks and Quantum Monte Carlo). N.S. and J.E.M. were supported by the U.S. Department of Energy, Office of Science, Office of Basic Energy Sciences, Materials Sciences and Engineering Division under Contract No. DE-AC02-05-CH11231 through the Theory Institute for Molecular Spectroscopy (TIMES). J.E.M. was also supported by a Simons Investigatorship. This research used the Lawrence computational cluster resource provided by the IT Division

at the Lawrence Berkeley National Laboratory (supported by the Director, Office of Science, Office of Basic Energy Sciences, of the U.S. Department of Energy under Contract No. DE-AC02-05CH11231). This research also used resources of the National Energy Research Scientific Computing Center (NERSC), a U.S. Department of Energy Office of Science User Facility operated under Contract No. DE-AC02-05CH11231.

-
- [1] F. D. M. Haldane, “Nonlinear field theory of large-spin Heisenberg antiferromagnets: Semiclassically quantized solitons of the one-dimensional easy-axis n el state,” *Phys. Rev. Lett.* **50**, 1153–1156 (1983).
- [2] Thierry Giamarchi, *Quantum physics in one dimension*, Vol. 121 (Clarendon press, Oxford, 2003).
- [3] T. Giamarchi, “Some experimental tests of tomonaga–luttinger liquids,” *Int. J. Mod. Phys. B* **26**, 1244004 (2012).
- [4] Keola Wierschem and Pinaki Sengupta, “Characterizing the haldane phase in quasi-one-dimensional spin-1 Heisenberg antiferromagnets,” *Mod. Phys. Lett. B* **28**, 1430017 (2014).
- [5] Bruno Bertini, Mario Collura, Jacopo De Nardis, and Maurizio Fagotti, “Transport in out-of-equilibrium XXZ chains: Exact profiles of charges and currents,” *Phys. Rev. Lett.* **117**, 207201 (2016).
- [6] Olalla A. Castro-Alvaredo, Benjamin Doyon, and Takato Yoshimura, “Emergent hydrodynamics in integrable quantum systems out of equilibrium,” *Phys. Rev. X* **6**, 041065 (2016).
- [7] Vir B. Bulchandani, Romain Vasseur, Christoph Karrasch, and Joel E. Moore, “Bethe-boltzmann hydrodynamics and spin transport in the XXZ chain,” *Phys. Rev. B* **97**, 045407 (2018).
- [8] L. D. Landau and E. M. Lifshitz, *Fluid Mechanics*, 2nd ed. (Butterworth-Heinemann, Oxford, 1987).
- [9] X. Zotos, F. Naef, and P. Prelovsek, “Transport and conservation laws,” *Phys. Rev. B* **55**, 11029–11032 (1997).
- [10] J. Sirker, “Spin diffusion and the anisotropic spin- $\frac{1}{2}$ Heisenberg chain,” *Phys. Rev. B* **73**, 224424 (2006).
- [11] J. Sirker, R. G. Pereira, and I. Affleck, “Conservation laws, integrability, and transport in one-dimensional quantum systems,” *Phys. Rev. B* **83**, 035115 (2011).
- [12] Toma  Prosen, “Open XXZ spin chain: Nonequilibrium steady state and a strict bound on ballistic transport,” *Phys. Rev. Lett.* **106**, 217206 (2011).
- [13] Marko  nidari , “Spin transport in a one-dimensional anisotropic Heisenberg model,” *Phys. Rev. Lett.* **106**, 220601 (2011).
- [14] C. Karrasch, J. Hauschild, S. Langer, and F. Heidrich-Meisner, “Drude weight of the spin- $\frac{1}{2}$ XXZ chain: Density matrix renormalization group versus exact diagonalization,” *Phys. Rev. B* **87**, 245128 (2013).
- [15] E. Ilievski, J. De Nardis, B. Wouters, J.-S. Caux, F. H. L. Essler, and T. Prosen, “Complete generalized gibbs ensembles in an interacting theory,” *Phys. Rev. Lett.* **115**, 157201 (2015).
- [16] Jacopo De Nardis, Denis Bernard, and Benjamin Doyon, “Hydrodynamic diffusion in integrable systems,” *Phys. Rev. Lett.* **121**, 160603 (2018).
- [17] Sarang Gopalakrishnan, David A. Huse, Vedika Khemani, and Romain Vasseur, “Hydrodynamics of operator spreading and quasiparticle diffusion in interacting integrable systems,” *Phys. Rev. B* **98**, 220303 (2018).
- [18] Jacopo De Nardis, Denis Bernard, and Benjamin Doyon, “Diffusion in generalized hydrodynamics and quasiparticle scattering,” *SciPost Phys.* **6**, 49 (2019).
- [19] Utkarsh Agrawal, Sarang Gopalakrishnan, and Romain Vasseur, “Generalized hydrodynamics, quasiparticle diffusion, and anomalous local relaxation in random integrable spin chains,” *Phys. Rev. B* **99**, 174203 (2019).
- [20] Marko Ljubotina, Marko  nidari , and Toma   Prosen, “Kardar-Parisi-Zhang physics in the quantum Heisenberg magnet,” *Phys. Rev. Lett.* **122**, 210602 (2019).
- [21] Jacopo De Nardis, Marko Medenjak, Christoph Karrasch, and Enej Ilievski, “Anomalous spin diffusion in one-dimensional antiferromagnets,” *Phys. Rev. Lett.* **123**, 186601 (2019).
- [22] Sarang Gopalakrishnan and Romain Vasseur, “Kinetic theory of spin diffusion and superdiffusion in XXZ spin chains,” *Phys. Rev. Lett.* **122**, 127202 (2019).
- [23] Sarang Gopalakrishnan, Romain Vasseur, and Brayden Ware, “Anomalous relaxation and the high-temperature structure factor of XXZ spin chains,” *Proc. Natl. Acad. Sci.* **116**, 16250–16255 (2019).
- [24] Maxime Dupont and Joel E. Moore, “Universal spin dynamics in infinite-temperature one-dimensional quantum magnets,” *Phys. Rev. B* **101**, 121106 (2020).
- [25] Jacopo De Nardis, Marko Medenjak, Christoph Karrasch, and Enej Ilievski, “Universality classes of spin transport in one-dimensional isotropic magnets: The onset of logarithmic anomalies,” *Phys. Rev. Lett.* **124**, 210605 (2020).
- [26] Jacopo De Nardis, Sarang Gopalakrishnan, Enej Ilievski, and Romain Vasseur, “Superdiffusion from emergent classical solitons in quantum spin chains,” *Phys. Rev. Lett.* **125**, 070601 (2020).
- [27] Aaron J. Friedman, Sarang Gopalakrishnan, and Romain Vasseur, “Diffusive hydrodynamics from integrability breaking,” *Phys. Rev. B* **101**, 180302 (2020).
- [28] Utkarsh Agrawal, Sarang Gopalakrishnan, Romain Vasseur, and Brayden Ware, “Anomalous low-frequency conductivity in easy-plane XXZ spin chains,” *Phys. Rev. B* **101**, 224415 (2020).
- [29] Enej Ilievski, Jacopo De Nardis, Sarang Gopalakrishnan, Romain Vasseur, and Brayden Ware, “Superuniversality of superdiffusion,” [arXiv:2009.08425](https://arxiv.org/abs/2009.08425) (2020).
- [30] Vir B. Bulchandani, “Kardar-Parisi-Zhang universality from soft gauge modes,” *Phys. Rev. B* **101**, 041411 (2020).
- [31] B. Bertini, F. Heidrich-Meisner, C. Karrasch, T. Prosen, R. Steinigeweg, and M. Znidaric, “Finite-temperature transport in one-dimensional quantum lattice models,” [arXiv:2003.03334](https://arxiv.org/abs/2003.03334) (2020).
- [32] Javier Lopez-Piqueres, Brayden Ware, Sarang Gopalakrishnan, and Romain Vasseur, “Hydrodynamics of nonintegrable systems from a relaxation-time approximation,” *Phys. Rev. B* **103**, L060302 (2021).
- [33] Jacopo De Nardis, Sarang Gopalakrishnan, Romain Vasseur, and Brayden Ware, “Stability of superdiffusion in nearly integrable spin chains,” [arXiv:2102.02219](https://arxiv.org/abs/2102.02219) (2021).
- [34] A. Scheie, N. E. Sherman, M. Dupont, S. E. Nagler, M. B. Stone, G. E. Granroth, J. E. Moore, and D. A. Tennant, “Detection of Kardar–Parisi–Zhang hydrodynamics in a quantum Heisenberg spin-1/2 chain,” *Nat. Phys.* (2021).
- [35] Elliott H. Lieb and Werner Liniger, “Exact analysis of an interacting bose gas. i. the general solution and the ground state,” *Phys. Rev.* **130**, 1605–1616 (1963).
- [36] Elliott H. Lieb, “Exact analysis of an interacting bose gas. ii. the excitation spectrum,” *Phys. Rev.* **130**, 1616–1624 (1963).
- [37] M. Schemmer, I. Bouchoule, B. Doyon, and J. Dubail, “Generalized hydrodynamics on an atom chip,” *Phys. Rev. Lett.* **122**, 090601 (2019).

- [38] Neel Malvania, Yicheng Zhang, Yuan Le, Jerome Dubail, Marcos Rigol, and David S. Weiss, “Generalized hydrodynamics in strongly interacting 1d bose gases,” [arXiv:2009.06651](https://arxiv.org/abs/2009.06651) (2020).
- [39] Paul Niklas Jepsen, Jesse Amato-Grill, Ivana Dimitrova, Wen Wei Ho, Eugene Demler, and Wolfgang Ketterle, “Spin transport in a tunable Heisenberg model realized with ultracold atoms,” *Nature* **588**, 403–407 (2020).
- [40] Mehran Kardar, Giorgio Parisi, and Yi-Cheng Zhang, “Dynamic scaling of growing interfaces,” *Phys. Rev. Lett.* **56**, 889–892 (1986).
- [41] K. R. Thurber, A. W. Hunt, T. Imai, and F. C. Chou, “¹⁷O NMR study of $q = 0$ spin excitations in a nearly ideal $S = \frac{1}{2}$ 1D Heisenberg antiferromagnet, Sr₂CuO₃, up to 800 K,” *Phys. Rev. Lett.* **87**, 247202 (2001).
- [42] Ulrich Schollwöck, “The density-matrix renormalization group in the age of matrix product states,” *Ann. Phys.* **326**, 96 – 192 (2011).
- [43] Matthew Fishman, Steven R. White, and E. Miles Stoudenmire, “The ITensor software library for tensor network calculations,” [arXiv:2007.14822](https://arxiv.org/abs/2007.14822) (2020).
- [44] F. Verstraete, J. J. García-Ripoll, and J. I. Cirac, “Matrix product density operators: Simulation of finite-temperature and dissipative systems,” *Phys. Rev. Lett.* **93**, 207204 (2004).
- [45] Michael Zwolek and Guifré Vidal, “Mixed-state dynamics in one-dimensional quantum lattice systems: A time-dependent superoperator renormalization algorithm,” *Phys. Rev. Lett.* **93**, 207205 (2004).
- [46] Guifré Vidal, “Efficient simulation of one-dimensional quantum many-body systems,” *Phys. Rev. Lett.* **93**, 040502 (2004).
- [47] Naomichi Hatano and Masuo Suzuki, “Finding exponential product formulas of higher orders,” in *Quantum Annealing and Other Optimization Methods*, edited by Arnab Das and Bikas K. Chakrabarti (Springer Berlin Heidelberg, Berlin, Heidelberg, 2005) pp. 37–68.
- [48] We use a Trotter step $\delta = 0.1$ leading to a negligible discretization error $O(\delta^5)$.
- [49] See Supplementary Information at [URL will be inserted by publisher] for a reanalysis of past NMR experiments on Sr₂CuO₃ from Ref. 41, compatible with superdiffusion ($z = 3/2$) and with $Y(T) \sim T^2$; details on the convergence with the system size L and the bond dimension χ ; a comparison between the real and imaginary parts of the spin-spin correlation function; additional zero temperature data and a discussion. See also Refs. [41–43, 46, 47, 50, 51, 55, 58, 59, 73] therein.
- [50] Rodrigo G. Pereira, Steven R. White, and Ian Affleck, “Exact edge singularities and dynamical correlations in spin-1/2 chains,” *Phys. Rev. Lett.* **100**, 027206 (2008).
- [51] Rodrigo G. Pereira, “Long time correlations of nonlinear luttinger liquids,” *Int. J. Mod. Phys. B* **26**, 1244008 (2012).
- [52] I Affleck, D Gepner, H J Schulz, and T Ziman, “Critical behaviour of spin-s Heisenberg antiferromagnetic chains: analytic and numerical results,” *J. Phys. A* **22**, 511–529 (1989).
- [53] Kiyohide Nomura and Miki Yamada, “Thermal bethe-ansatz study of the correlation length of the one-dimensional s=1/2 Heisenberg antiferromagnet,” *Phys. Rev. B* **43**, 8217–8223 (1991).
- [54] Sebastian Eggert, Ian Affleck, and Minoru Takahashi, “Susceptibility of the spin 1/2 Heisenberg antiferromagnetic chain,” *Phys. Rev. Lett.* **73**, 332–335 (1994).
- [55] M. Takigawa, O. A. Starykh, A. W. Sandvik, and R. R. P. Singh, “Nuclear relaxation in the spin-1/2 antiferromagnetic chain compound Sr₂CuO₃: Comparison between theories and experiments,” *Phys. Rev. B* **56**, 13681–13684 (1997).
- [56] Ian Affleck, “Exact correlation amplitude for the Heisenberg antiferromagnetic chain,” *J. Phys. A* **31**, 4573–4581 (1998).
- [57] Victor Barzykin, “Temperature-dependent logarithmic corrections in the spin-1/2 Heisenberg chain,” *J. Condens. Matter Phys.* **12**, 2053–2059 (2000).
- [58] Victor Barzykin, “NMR relaxation rates in a spin- $\frac{1}{2}$ antiferromagnetic chain,” *Phys. Rev. B* **63**, 140412 (2001).
- [59] Maxime Dupont, Sylvain Capponi, and Nicolas Laflorencie, “Temperature dependence of the NMR relaxation rate $1/T_1$ for quantum spin chains,” *Phys. Rev. B* **94**, 144409 (2016).
- [60] Herbert Spohn, “Fluctuating hydrodynamics approach to equilibrium time correlations for anharmonic chains,” in *Thermal Transport in Low Dimensions* (Springer, 2016) pp. 107–158.
- [61] Michael Prähofer and Herbert Spohn, “Exact scaling functions for one-dimensional stationary KPZ growth,” *J. Stat. Phys.* **115**, 255–279 (2004).
- [62] M. Klanjšek, H. Mayaffre, C. Berthier, M. Horvatić, B. Chiari, O. Piovesana, P. Bouillot, C. Kollath, E. Orignac, R. Citro, and T. Giamarchi, “Controlling luttinger liquid physics in spin ladders under a magnetic field,” *Phys. Rev. Lett.* **101**, 137207 (2008).
- [63] Pierre Bouillot, Corinna Kollath, Andreas M. Läuchli, Mikhail Zvonarev, Benedikt Thielemann, Christian Rüegg, Edmond Orignac, Roberta Citro, Martin Klanjšek, Claude Berthier, Mladen Horvatić, and Thierry Giamarchi, “Statics and dynamics of weakly coupled antiferromagnetic spin- $\frac{1}{2}$ ladders in a magnetic field,” *Phys. Rev. B* **83**, 054407 (2011).
- [64] M. Jeong, H. Mayaffre, C. Berthier, D. Schmidiger, A. Zheludev, and M. Horvatić, “Attractive tomonaga-luttinger liquid in a quantum spin ladder,” *Phys. Rev. Lett.* **111**, 106404 (2013).
- [65] M. Jeong, D. Schmidiger, H. Mayaffre, M. Klanjšek, C. Berthier, W. Knafo, G. Ballon, B. Vignolle, S. Krämer, A. Zheludev, and M. Horvatić, “Dichotomy between attractive and repulsive tomonaga-luttinger liquids in spin ladders,” *Phys. Rev. Lett.* **117**, 106402 (2016).
- [66] E. Coira, P. Barmettler, T. Giamarchi, and C. Kollath, “Temperature dependence of the NMR spin-lattice relaxation rate for spin- $\frac{1}{2}$ chains,” *Phys. Rev. B* **94**, 144408 (2016).
- [67] Claude Berthier, Mladen Horvatić, Marc-Henri Julien, Hadrien Mayaffre, and Steffen Krämer, “Nuclear magnetic resonance in high magnetic field: Application to condensed matter physics,” *2016 Prizes of the French Academy of Sciences /Prix 2016 de l’Académie des sciences, C. R. Phys.* **18**, 331–348 (2017).
- [68] Maxime Dupont, Sylvain Capponi, Nicolas Laflorencie, and Edmond Orignac, “Dynamical response and dimensional crossover for spatially anisotropic antiferromagnets,” *Phys. Rev. B* **98**, 094403 (2018).
- [69] Mladen Horvatić, Martin Klanjšek, and Edmond Orignac, “Direct determination of the tomonaga-luttinger parameter k in quasi-one-dimensional spin systems,” *Phys. Rev. B* **101**, 220406 (2020).
- [70] Anatole Abragam and HY Carr, *The principles of nuclear magnetism* (Clarendon Press, Oxford, UK, 1961).
- [71] Mladen Horvatić and Claude Berthier, “NMR Studies of Low-Dimensional Quantum Antiferromagnets,” in *High Magnetic Fields*, Lecture Notes in Physics No. 595, edited by C. Berthier, L. P. Lévy, and G. Martinez (Springer Berlin Heidelberg, 2002) pp. 191–210.
- [72] Charles P Slichter, *Principles of magnetic resonance*, Vol. 1 (Springer Science & Business Media, Berlin, Heidelberg, 2013).
- [73] Steven R. White, “Density matrix formulation for quantum renormalization groups,” *Phys. Rev. Lett.* **69**, 2863–2866 (1992).

Supplementary Information for “Spatiotemporal crossover between low- and high-temperature dynamical regimes in the quantum Heisenberg magnet”

First, we revisit past NMR measurements for the nearly-ideal spin-1/2 Heisenberg chain Sr_2CuO_3 . We show that these results, which were interpreted in the context of diffusion, are compatible with the current understanding of the high-temperature dynamics of the one-dimensional $S = 1/2$ Heisenberg model, which is known to be superdiffusive. Second, we provide additional data to understand the convergence of the numerical simulation with respect to the control parameter (namely the bond dimension of the matrix product state χ) and the system size L . Third, we show that the real part of the dynamical spin-spin correlation function dominates the imaginary part and that the real part hosts the characteristic power-law dependence $\propto t^{-2/3}$. Finally, we present additional numerical results at exactly zero temperature to connect our low-temperature data to zero temperature dynamics.

I. REVISITING EXPERIMENTAL NMR DATA FOR Sr_2CuO_3

A. Characterizing anomalous spin transport

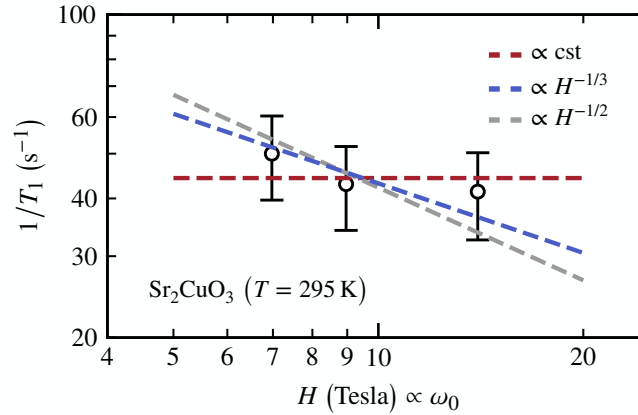


FIG. S1. The data reported on this figure is extracted from Fig. 3(d) of Ref. 41. It corresponds to the NMR relaxation rate $1/T_1$ versus the strength of the applied external magnetic field H for Sr_2CuO_3 at $T = 295$ K (the exchange coupling is $J \simeq 2200$ K). The NMR was performed on the ^{17}O nuclei, coupled symmetrically to the Cu^{2+} ions carrying the relevant electronic spins $S = 1/2$. As a result, the NMR relaxation rate $1/T_1$ filters out $q = \pm\pi$ components but conserves nonetheless the long-wavelength modes $q = 0$ holding hydrodynamics. The applied field is directly proportional to the NMR frequency ω_0 as per the Zeeman splitting.

We revisit in Fig. S1 the experimental data of Fig. 3(d) in Ref. 41. In this work, a power-law behavior of the form $1/T_1 \propto H^{-\alpha}$ assuming $\alpha = 0.5$ (corresponding to diffusion) was reported for the nearly ideal spin-1/2 Heisenberg antiferromagnets Sr_2CuO_3 . Here, in addition to the diffusive behavior, we show the best superdiffusive fit of the form $\propto H^{-1/3}$, which is the expected behavior for the quantum spin-1/2 Heisenberg chain, based on today’s knowledge. We also show the best constant fit of the form $\propto H^0$ corresponding to ballistic transport.

From a purely theoretical perspective, we expect ballistic spin transport in the infinite time limit due to the external magnetic field. However, the magnetic field being extremely small (14 T) compared to the spin exchange coupling in this compound ($J \simeq 2200$ K), the crossover might happen beyond the timescale related to the NMR frequency, making the dynamics look effectively super-diffusive. The effect of the magnetic field needs to be precisely studied and we leave that for future work. For instance, for the low-energy physics studied in Refs. 41 and 55, the effect of the magnetic field was irrelevant.

In any case, three data points are not enough to unambiguously identify the correct behavior, calling for new and dedicated NMR experiments on the issue of anomalous spin transport in one-dimensional spin chains. In particular, we believe that the present numerical abilities to efficiently simulate the microscopic dynamics of interacting 1D quantum models could greatly help in guiding experiments.

B. The behavior $\Upsilon(T) \propto T^2$ for $T \ll J$ is compatible with experimental observations

We approximate the real part of the spin-spin correlation $\Re C(T, x = 0, t)$ by $\Upsilon(T)t^{-2/3}$, which is the correct behavior in the long-time limit, see Fig. 2 in the main text. We get for the NMR relaxation rate,

$$\frac{1}{T_1} \sim \int_0^{1/\omega_0} \Re C(T, x = 0, t) dt \sim \Upsilon(T)\omega_0^{-1/3} \implies \frac{1}{T_1} \sim T^2\omega_0^{-1/3} \text{ for } T \ll J, \quad (\text{S1})$$

where we found that $\Upsilon(T) \sim T^2$ for $T \ll J$, see Fig. 3(b) in the main text. As discussed in the main text, $\Upsilon(T)$ relates to the temperature dependence of the parameters of the KPZ equation: $\frac{\sigma^2}{2\nu}(\sqrt{2}\lambda)^{-2/3}f_{\text{KPZ}}(0) \sim \Upsilon(T)$.

In Fig. 4(a) of Ref. 41, the authors find that for $T \ll J$, the NMR relaxation rate of Sr_2CuO_3 at fixed frequency ω_0 may be approximated by an empirical form $1/T_1 \approx aT + bT^2$ for $T \ll J$ with a and b fitting constants. Up to the term with linear temperature dependence aT , this is the behavior obtained in Eq. (S1).

Neglecting the experimental data points for very low temperatures ($T \lesssim 100$ K), the experimental data of Fig. 4(a) in Ref. 41 is compatible with $1/T_1 \sim T^2$. Substituting the real part of the correlator by its asymptotic behavior in Eq. (S1) becomes less and less valid at very low temperatures: the low-temperature physics of the real part of the correlator, not taken into account in the approximation of Eq. (S1) becomes dominant over high-temperature superdiffusive regime. In other words, in the time window $t \in [0, 1/\omega_0]$, the two regimes coexist with the low-temperature one for $t \lesssim t^*$ and the high-temperature one for $t \gtrsim t^*$, with $t^* \sim 1/T$ (see main text). In Eq. (S1), it is assumed that the high-temperature regime is dominant. In this picture, we interpret the small flattening observed for very low temperatures ($T \lesssim 100$ K) in Fig. 4(a) of Ref. 41, and which gives rise to the linear term aT , as the onset of low-temperature physics characterized by $1/T_1 \approx \ln^{-1/2}(J/T)$ [55, 58, 59]. In fact, this logarithmic divergence was reported in Ref. 55 for the same compound (Sr_2CuO_3) for temperatures $T/J \lesssim 0.05$, corresponding to $T \approx 100$ K, i.e., the regime where a linear term aT is necessary to fit the experimental $1/T_1$ data.

For these reasons, we believe that the behavior $1/T_1 \sim T^2$ reported in Eq. (S1) is compatible with earlier experimental measurements on Sr_2CuO_3 [41], and relates to the temperature dependence of the parameters of the KPZ equation.

II. BOND DIMENSION CONVERGENCE OF THE NUMERICAL SIMULATIONS

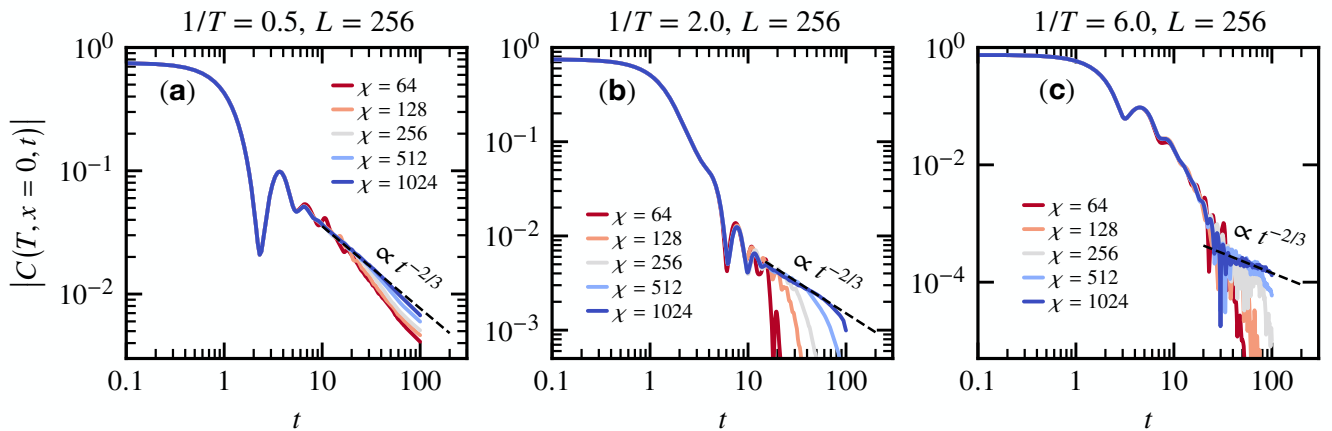


FIG. S2. Time dependence of the norm of the spin-spin correlation of Eq. 2 in the main text at $x = 0$ for various values of the bond dimension $\chi = 64, 128, 256, 512,$ and 1024 . Simulations obtained for $L = 256$ at three different temperatures (a) $1/T = 0.5$, (b) $1/T = 2.0$, and (c) $1/T = 6.0$. At long time, it displays an algebraic decay $\propto t^{-2/3}$ (dashed black line).

To understand the effect of the finite bond dimension χ on the numerical simulation, we performed the same calculations for $\chi = 64, 128, 256, 512,$ and 1024 (the larger, the better, and results in the main text correspond to $\chi = 1024$). As one increases the bond dimension, the numerical data gets closer and closer to the expected $\propto t^{-2/3}$ power-law dependence at long-time, see Fig. S2.

III. SYSTEM SIZE CONVERGENCE OF THE NUMERICAL SIMULATIONS

By plotting data for increasing system sizes for the spin-spin correlation of Eq. 2 in the main text at $x = 0$, we see in Fig. S3 that finite-size effects only take place at times $t \approx L/2$, reminiscent of the light-cone structure (data available for up to $L = 256$). Data at $|x| > 0$ in Fig. 4 of the main text are shown up to $|x| = 25$, which is still far away from the system boundary at $|x| = 128$. Therefore, the conclusions drawn in the manuscript are independent of the system size.

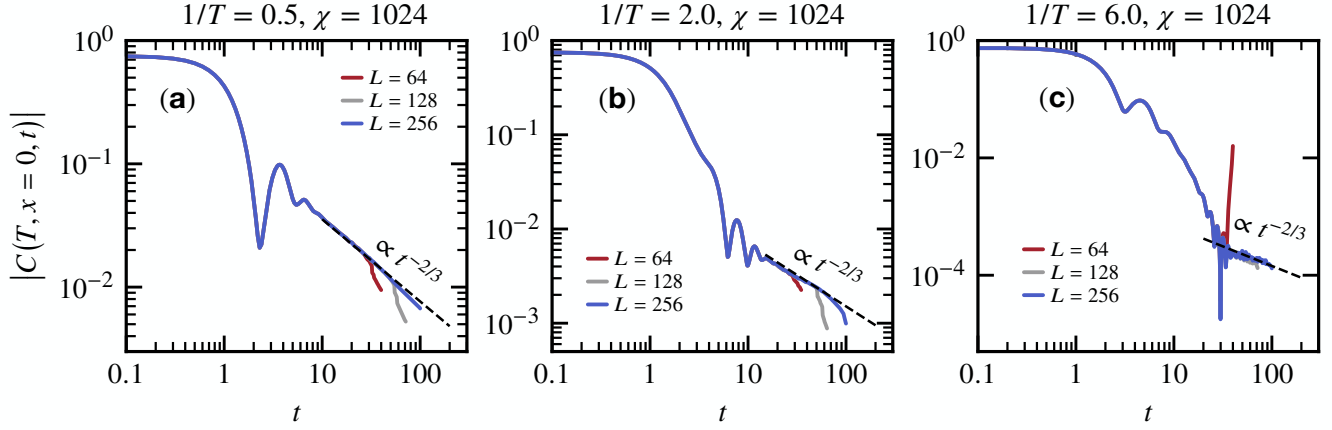


FIG. S3. Time dependence of the norm of the spin-spin correlation of Eq. 2 in the main text at $x = 0$ for various system sizes $L = 64, 128$, and 256 . Simulations obtained for a bond dimension $\chi = 1024$ at three different temperatures (a) $1/T = 0.5$, (b) $1/T = 2.0$, and (c) $1/T = 6.0$. At long time, it displays an algebraic decay $\propto t^{-2/3}$ (dashed black line).

IV. REAL PART VERSUS IMAGINARY PART OF THE DYNAMICAL SPIN-SPIN CORRELATION

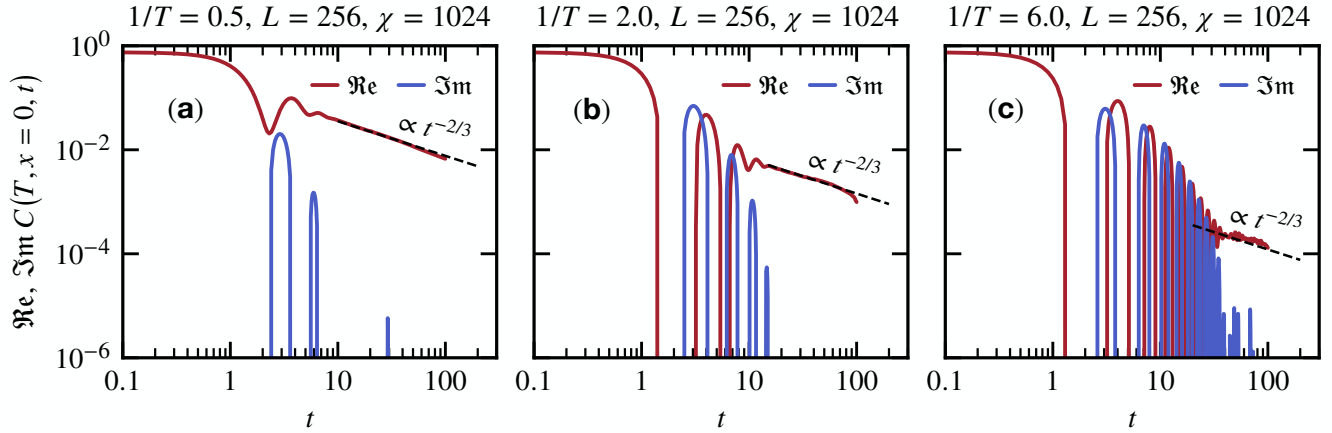


FIG. S4. Time dependence of the real part “ \Re ” and imaginary part “ \Im ” part of the spin-spin correlation of Eq. 2 in the main text at $x = 0$. Simulations obtained for $L = 256$ and $\chi = 1024$ at three different temperatures (a) $1/T = 0.5$, (b) $1/T = 2.0$, and (c) $1/T = 6.0$. We observe that the superdiffusive power-law regime $\propto t^{-2/3}$ only holds for the real part (dashed black line) and that in this regime we have $|\Im C(T, x = 0, t)| \ll |\Re C(T, x = 0, t)|$.

While we display the norm of the spin-spin correlation function in the main text, we compute both the real and imaginary parts. We show them independently in Fig. S4. We observe that the real part hosts the characteristic power-law dependence $\propto t^{-2/3}$, not the imaginary part. In fact, in the hydrodynamics regime, we find that $|\Im C(T, x, t)| \ll |\Re C(T, x, t)|$, meaning that at long time, the imaginary part plays no role in the superdiffusive dynamics of the spin-1/2 Heisenberg chain.

V. LOW-TEMPERATURE VERSUS ZERO TEMPERATURE

By plotting the different system sizes for the spin-spin correlation of Eq. 2 in the main text at $x = 0$ and $T = 0$, see Fig. S5(e) we show that the “flattening” observed at long times is a finite size effect. In Figs. S5(a)–S5(d) we show the effect of the finite bond dimension, which is qualitatively very small.

Our data confirm the $\propto 1/t$ decay (up to logarithmic corrections) of the $x = 0$ spin-spin correlation at zero temperature for the spin-1/2 Heisenberg chain [50, 51] in Fig. S5(e). We also confirm that the finite-temperature data (down to $1/T = 7.0$ in the main text) is actually not small enough to observe the genuine low-temperature dynamics. We see in Fig. S6 that at least $1/T \gtrsim 20.0$ is required to have an overlap between zero-temperature and finite-temperature data in a reasonable time window.

Note that the numerical simulations for zero temperature $T = 0$ are carried out with a slightly different method than for $T > 0$. In particular, we do not need to use the trick representing a mixed state as a pure state in an enlarged Hilbert space, the state at $T = 0$ being a pure state (it is the ground state). The ground state is obtained with the density matrix renormalization group algorithm [42, 43, 73], and the time evolution is then performed using time-evolving block decimation algorithm [46] along with a fourth-order Trotter decomposition [47] with step $\delta = 0.1$ leading to a negligible discretization error $O(\delta^5)$.

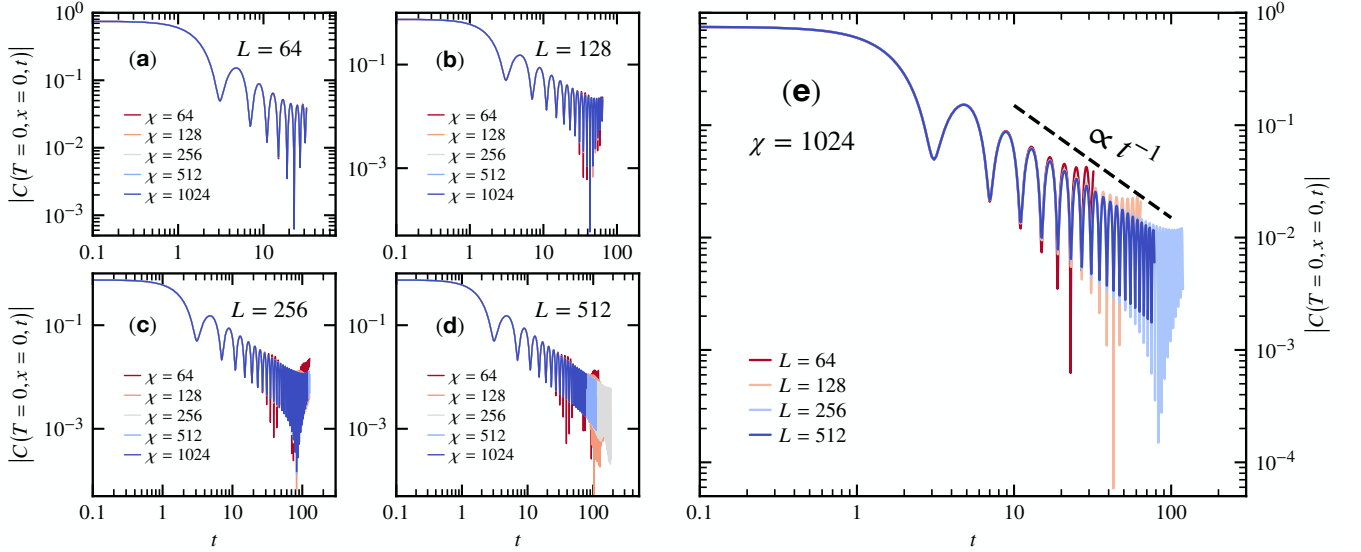


FIG. S5. Time dependence of the norm of the spin-spin correlation of Eq. 2 in the main text at $x = 0$ for various system sizes $L = 64, 128$, and 256 and bond dimensions $\chi = 64, 128, 256, 512$, and 1024 at zero temperature ($T = 0$). (a) $L = 64$, (b) $L = 128$, (c) $L = 256$, and (d) $L = 512$ for various bond dimensions χ . (e) $\chi = 1024$ for various system sizes L .

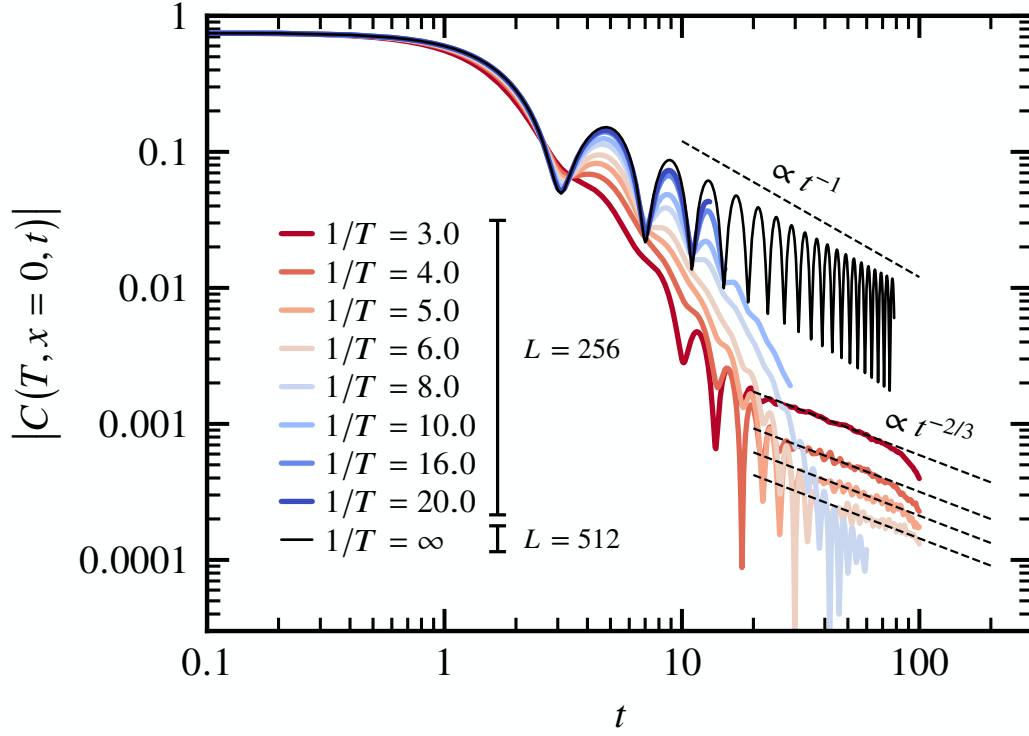


FIG. S6. Time dependence of the norm of the spin-spin correlation of Eq. 2 in the main text at $x = 0$ for various temperatures T . Simulations obtained for $L = 256$ with $\chi = 1024$ at finite temperature and for $L = 512$ with $\chi = 1024$ at zero temperature. Same data as in Fig. 2 of the main text plus the zero temperature ($1/T = \infty$), $1/T = 8.0$, $1/T = 10.0$, $1/T = 16.0$, and, $1/T = 20.0$ data.